International Journal for Computational Civil and Structural Engineering, 18(1) 109–118 (2022)

DOI:10.22337/2587-9618-2022-18-1-109-118

ON THE LOSS OF STABILITY AND POSTCRITICAL EQUILIBRIUM OF COMPRESSED THIN-WALLED ANGLE BARS

Gaik A. Manuylov, Sergey B. Kosytsyn, Maxim M. Begichev

Russian University of Transport, Moscow, RUSSIA

Abstract: Angle bars in compression are quite common in building and transport structures. However, the peculiarities of their behavior during the loss of stability and in supercritical equilibrium have not been sufficiently studied even within the limits of elastic deformations. The paper shows solutions for the stability of symmetric and asymmetric rods with an angle profile. The development of post-critical deformations is shown. The features of the behavior of the rods, obeying the hypotheses of V.Z. Vlasov.

Keywords: stability, geometric nonlinearity, finite element method, angle bar, buckling.

О ПОТЕРЕ УСТОЙЧИВОСТИ И ЗАКРИТИЧЕСКОМ РАВНОВЕСИИ СЖАТЫХ ТОНКОСТЕННЫХ СТЕРЖНЕЙ УГОЛКОВОГО ПРОФИЛЯ

Г.А. Мануйлов, С.Б. Косицын, М.М. Бегичев

Российский университет транспорта, г. Москва, РОССИЯ

Аннотация: Стержни уголкового профиля, работающие на сжатие, довольно часто встречаются в строительных и транспортных конструкциях. Однако особенности их поведения при потере устойчивости и в закритическом равновесии изучены недостаточно даже в пределах упругих деформаций. В работе приведены расчеты на устойчивость симметричных и несимметричных стержней с уголковым профилем. Показано развитие послекритических деформаций. Показаны особенности поведения стержней, подчиняющегося гипотезам В.З. Власова.

Ключевые слова: устойчивость, геометрическая нелинейность, метод конечных элементов, стержни уголкового сечения, потеря устойчивости.

Angle bars in compression are quite common in building and transport structures [1-3]. However, the peculiarities of their behavior during the loss of stability and in supercritical equilibrium have not been sufficiently studied even within the limits of elastic deformations. In this case, the choice of the examined model of the beam turns out to be essential [4-8]. There are two options here:

1) The beam is considered as thin-walled, complying with the hypotheses of V.Z. Vlasov [8];

2) The beam is examined without the stiffening hypotheses of Vlasov.

The analysis of its equilibrium states is carried out numerically, using the FEM, taking into account the effects of geometric nonlinearity [9].

Examining the model of a thin-walled Vlasov rod by M. Pignataro and his collaborators [10, 11] using the expansion of the total potential energy up to cubic terms, and investigating the possibility of making the slope angle of the bifurcation curve vanish at the bifurcation point, obtained the necessary conditions for the stability of the supercritical equilibrium of the thin-walled beams in general and of the angle bars, in particular. The authors of this work numerically investigated the angle bars from the M. Pignataro's work (and those close to them in geometry). However, slightly different results were obtained.

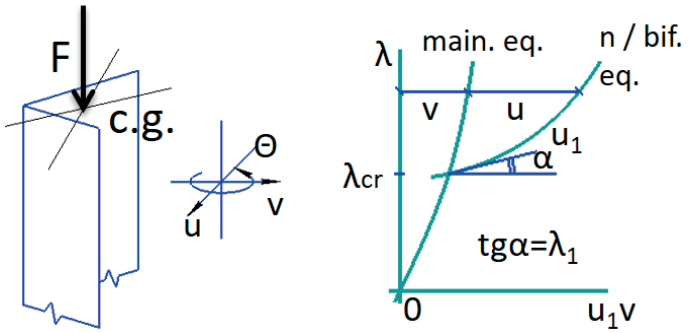

Figure 1. Branching of bifurcation curve

First, let us briefly outline the results of M. Pignataro and his co-workers concerning the stability of the thin-walled Vlasov beams supercritical equilibrium.

We assume that the curve of the "new" post-bifurcation equilibrium $\lambda(v)$ branches off from the curve of the basic equilibrium λ (ν) at the bifurcation point $(\lambda = \lambda_{cr})$ (Fig. 1). The parametric representation of the curves λ (ε) and $u(\varepsilon)$ gives the expansions

$$\lambda(\varepsilon) = \lambda_{cr} + \lambda_1 \varepsilon + \lambda_2 \varepsilon^2/_2 + \cdots$$
$$u(\varepsilon) = 0 + \dot{u}\varepsilon + \ddot{u}/_2 \varepsilon^2 + \cdots$$

The dots above denote derivatives with respect to ε; the subscripts correspond to the derivatives with respect to the coordinate. Here, the proper form $v_1 = \dot{u}$, the potential energy in critical equilibrium is

$$P_c(u) = \frac{1}{2} P_c'' u^2 + \frac{1}{6} P_c''' u^3 + \cdots$$

The slope of the tangent to the curve of the "new" equilibria at the bifurcation point is λ_1 [10, 11] (Fig. 1)

$$\lambda_1 = tg\ \alpha = -P_c''' u_1^3 / 2\dot{P}_c'' u_1^2$$

If $\lambda_1 = tg\ \alpha \neq 0$, then the bifurcation diagram is asymmetric and the supercritical equilibrium is unstable. The system will be sensitive to initial imperfections.

On the contrary, the necessary condition for the stability of the initial post-bifurcation equilibrium is the equality to zero λ_1. This is possible if the cubic term is zero.

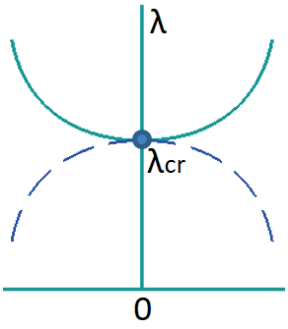

Figure 2. Symmetrical stable bifurcation diagram

$$P_c''' u_1^3 = 0$$

Then the bifurcation diagram is symmetric. It will determine a stable initial post-bifurcation equilibrium if the curvature of the curve of the "new" equilibrium is positive $(\lambda_2 > 0)$, where [10, 11] (Fig. 2)

$$\lambda_2 = \frac{\frac{1}{3} P_c'''' u_1^4 + P_c''' u_1^2 v_2}{\dot{P}_c'' u_1^2}, \text{ (for } \lambda_1 = 0)$$

The expression for the cubic term $\frac{1}{6} P_c''' v_1^3$ according to M. Pignataro is

$$\frac{1}{6} P_c''' u_1^3 = -\frac{1}{2} \int_0^l EI_{c\omega} \theta''(\theta')^2 + EI_{cx} u''(\theta')^2 + EI_{cy} v''(\theta')^2 - EI_x u' v' \theta' + EI_y v' u' \theta' | dz$$

Where $I_{c\omega}$, I_{cx}, I_{cy} are known integral geometric characteristics of a thin-walled beam section.
Under hinged boundary conditions at the ends of the beam, the eigenform is determined by a sinusoid with amplitudes $A_u, A_v \; and \; A_\theta$

$$u_1 = \dot{u}_c = [A_u, A_v, A_\theta] \sin {}^{\pi z}/_{l}$$

The expression for the cubic term in the expansion of the potential energy in terms of these amplitudes of its own form is

$$\frac{1}{6} P_c \dot{u}_1^3 = \frac{\pi^2 E}{3l^2} \left[I_{c\omega} A_\theta^3 + \left(I_{cx} A_v + I_{cy} A_u \right) A_\theta^2 + 2\left(I_y - I_x \right) A_u A_v A_\theta \right]$$

This expression is valid for any asymmetrical section. Therefore, for such a section, the cubic term is not equal to zero

$$\frac{1}{3} P_c''' u_1^3 \neq 0,$$

If $I_{c\omega} A_\theta^3 \neq 0$, or $I_{cx} A_v A_\theta^2 \neq 0$, or $I_{cy} A_u A_\theta^2 \neq 0$, or $\left(I_y - I_x \right) A_u A_v A_\theta \neq 0$. It turns out that a thin-walled hinged Vlasov beam with an asymmetric section has an unstable initial post-bifurcation equilibrium and will be sensitive to initial imperfections.
If the beam has one axis of symmetry and λ_{1c} is the critical buckling load in this plane, and λ_{2c} and λ_{3c} are the critical loads of flexural-torsional loss of stability from the symmetry plane, then for simple (not multiple) critical loads ($\lambda_{1c} \neq \lambda_{2c} \neq \lambda_{3c}$), or if $\lambda_{2c} = \lambda_{3c}$ the cubic term of the expansions is equal to zero ($P_c''' u_1^3 = 0$). Therefore, the bifurcation diagram is symmetric (and, most likely, stable). This is explained by the fact that in this case the amplitudes of the eigenmodes are

$$u_1^a = \begin{bmatrix} 0 \\ A_{v1} \\ 0 \end{bmatrix}, u_2^a = \begin{bmatrix} A_{u2} \\ 0 \\ A_{\theta 2} \end{bmatrix}, u_3^a = \begin{bmatrix} A_{u3} \\ 0 \\ A_{\theta 3} \end{bmatrix}$$

Since due to the symmetry

$$I_{c\omega} = I_{cx} = 0; \; I_{cy} \neq 0$$

then

$$\frac{1}{6} P_c u_1^3 = -\frac{\pi^2 E}{3l^2} \left[I_{cy} A_v A_\theta^2 + 2\left(I_y - I_x \right) A_u A_v A_\theta \right]$$

This expression equals to zero because there is no eigenform with all non-zero components.
If $\lambda_{1c} = \lambda_{2c}$ or $\lambda_{1c} = \lambda_{3c}$, then there is an eigenform u_{*c} in the form of a linear combination of u_{1c} and u_{2c} or u_{1c} and u_{3c}, which can have all components that are not equal to zero

$$u_{*c} = \begin{bmatrix} cA_{u2} \\ A_{v2} \\ cA_{\theta 2} \end{bmatrix} \neq 0$$

Then $\frac{1}{3} P_c''' u_*^3 \neq 0$, and the supercritical equilibrium of a beam with one symmetry plane will be unstable. The bifurcation diagram is asymmetric, and such a beam will be sensitive to initial imperfections.
Finally, if the beam section has two symmetry axes, then

$$I_{c\omega} = I_{cx} = I_{cy} = 0$$

and the expression for the cubic term is greatly simplified

$$\frac{1}{6} P_c''' u_1^3 = \frac{\pi^2 E}{3l^2} \left(I_y - I_x \right) A_u A_v A_\theta$$

The eigenforms' aplitudes

$$u_1^a = \begin{bmatrix} A_u \\ 0 \\ 0 \end{bmatrix}, u_2^a = \begin{bmatrix} 0 \\ A_v \\ 0 \end{bmatrix}, u_3^a = \begin{bmatrix} 0 \\ 0 \\ A_\theta \end{bmatrix}$$

For simple critical loads, it is obvious that $P_c''' u_1^3 = 0$ and the bifurcation diagram is symmetric. If $\lambda_{1c} = \lambda_{2c} = \lambda_{3c}$, then an eigenform with all nonzero components is possible in the form of a linear combination.

$$u_* = c_1 u_{1c} + c_2 u_{2c} + c_3 u_{3c} = \begin{bmatrix} c_1 A_u \\ c_2 A_v \\ c_3 A_\theta \end{bmatrix} \neq 0 \neq 0 \neq 0$$

Then the product $A_u A_v A_\theta \neq 0$. However, multiple critical loads are possible only when $I_y - I_x = 0$. Because of this, $P_c''' u_*^3 = 0$, and the bifurcation diagram of a beam with 2 planes of symmetry is always symmetric. Intuitively, it seems that this diagram also always determines a stable initial supercritical equilibrium. However, a rigorous proof requires considering an explicit expression for the quartic term $\frac{1}{24} P'''' u_1^4$. M. Pignataro and his collaborators gave [10, 11] several examples of imperfection sensitivity curves for beams with a section in the form of an equal- and unequal-angle bar, as well as with a section in the form of a T-beam. The dimensions of the one-axis symmetry beams were selected so that the corresponding critical loads were twofold. Initial imperfections are sinusoidal bends with amplitudes α, β, γ. These imperfections were specified in various combinations (Fig. 3, 4). For a bar with a cross-section in the form of an equal-angle bar, the largest drop in critical loads caused imperfection with the same amplitudes in all directions (Fig. 4).

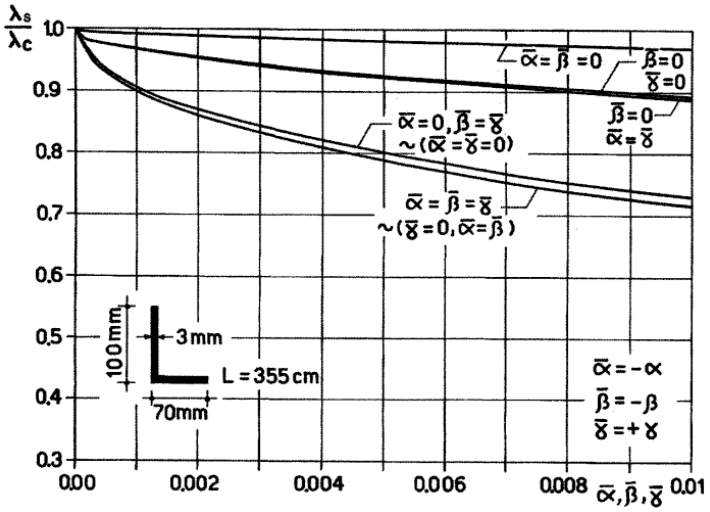

Figure 3. Dependence of critical loads on the values of combinations of initial imperfections for an asymmetric angle bar

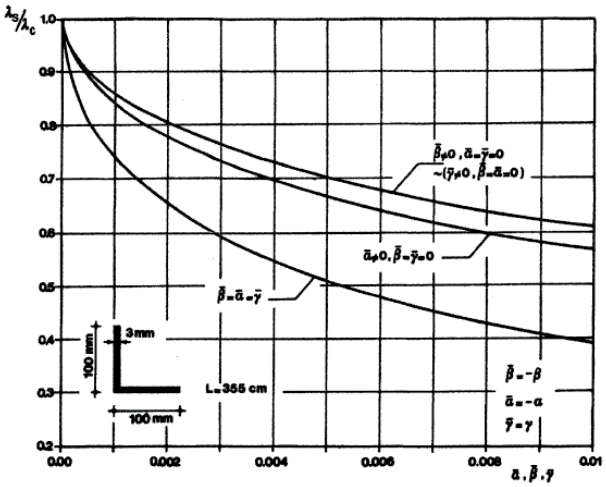

Figure 4. Dependence of critical loads on the values of combinations of initial imperfections for a symmetric angle bar

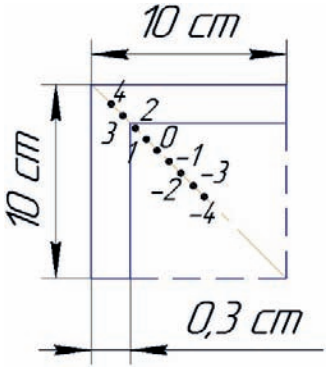

Figure 5. Cross-section of the beam

The authors of this work investigated the post-critical equilibrium of a hinged beam 355 cm long with a cross-section in the form of an equal-angle bar 10 × 10 × 0.3 cm. Such a beam was also studied by M. Pignataro and his collaborators, but as one by Vlasov.

There were rigid plates at the ends of the beam, which did not interfere with the rotation of the end sections. The compressive force was applied along the axis of the section symmetry (at the center of gravity or with an eccentricity of displacement Δe = 0.8 cm, Fig. 5).

Linear calculation of critical loads showed that the first two of them are quite close to each other (torsional $P_{cr\,1} = 39{,}3\ kN$, bending Euler $P_{cr2} = 39{,}34\ kN$). It would seem that the mutual influence of the corresponding closely related forms should significantly affect the beam's post-critical behavior.

However, similar beams of a different length (250 cm, 405 cm) with simple first critical loads showed equilibrium diagrams similar in character to the equilibrium diagram of a beam 355 cm long (Fig. 6). According to this figure, when the compressive load is displaced from the gravity center along the symmetry axis towards the edge (i.e., 1, 2, 3, and 4), the transverse displacements develop smoothly until the limit points are reached. After that, the deformation of "flattening" of the corner section begins to develop on the unstable branch. In this case, the flanges of the corner do not experience additional compression.

When the load shifts towards the center of the geometric contour 10×10 cm (points -1, -2, -3, -4, Fig. 5, 6), then there is a catastrophic drop in the maximum values of the compressive load due to the local loss of stability development of the corner flanges as compressed plates with free edges (Fig. 7).

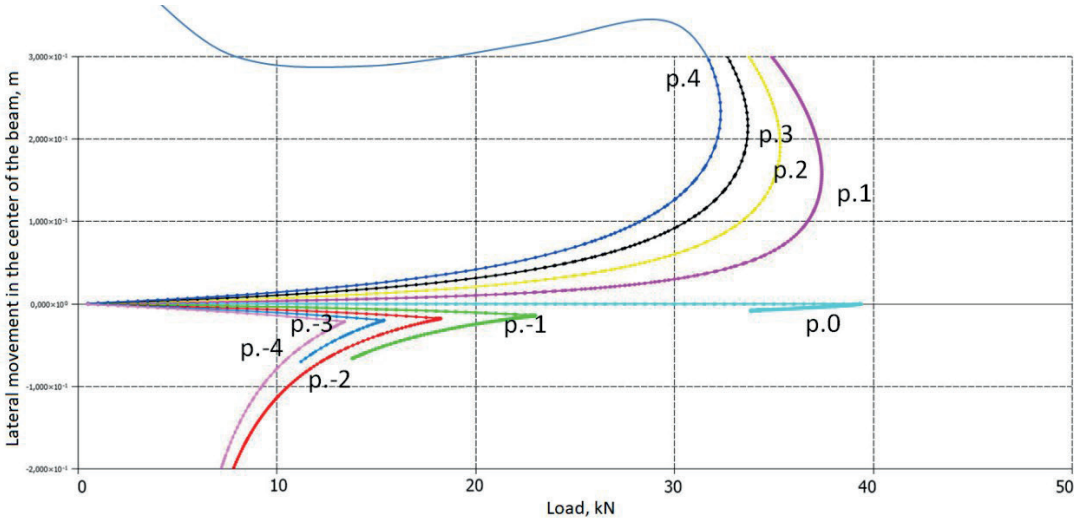

Figure 6. Deformation curves of symmetric angle bar (355 cm) under compression

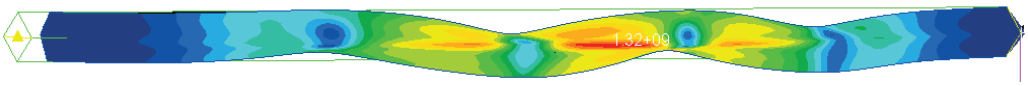

Figure 7. Local loss of stability of flanges

The obtained result testifies to the extreme sensitivity of angle bars to the location of the concentrated compressive load application point. When displaced diagonally from the center of gravity by 3.48 cm, the maximum load decreased by 3 times in comparison with the bifurcation one (Fig. 8). This is an unpleasant result of the buckling shapes interaction for engineers. If a concentrated compressive force must be applied at the point of the angle symmetry axis, then this point can only be between the edge and the angle section gravity center.

For a similar angle bar of a smaller length (l = 250 cm, Fig. 9), the nature of the equilibrium diagrams will not change.

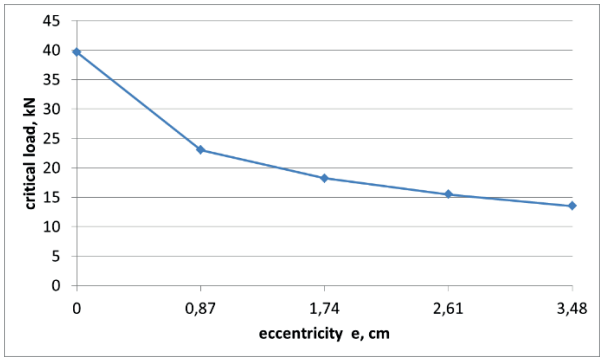

Figure 8. Influence of the location of compressive load application point for a symmetric angle bar on the critical loads

Only the maximum loads at the limiting points increased significantly when the force P was shifted towards the edge. But for such a beam, the critical forces are simple, and they differ significantly from each other.

For a longer rod (l = 405 cm) with the same cross-section, the first critical force $P_{cr\,1} = 31{,}55\ kN$ determines the bending form of buckling, and only the tenth one ($P_{cr\,10} = 37{,}85\ kN$) corresponds to the torsional loss of stability form. The maximum loads at the limiting points decreased slightly. However, the nature of the maximum loads fall at the moment of wave formation did not change ($^{\max P_{-4}}/_{\max P_0} = {}^{12{,}5}/_{32} = 0{,}39$).

Finally, let us consider the effect of transverse diaphragms (from 1 to 15) on the character of the hinged angle bar 355 cm long equilibrium curves (Fig. 10). This was an attempt to successively transform the FE-model of a "usual" beam into a Vlasov beam model with an invariable contour. With three or more diaphragms (Fig. 10), the maximum critical load of the central beam slightly increased (up to ~ 41.5 kN).

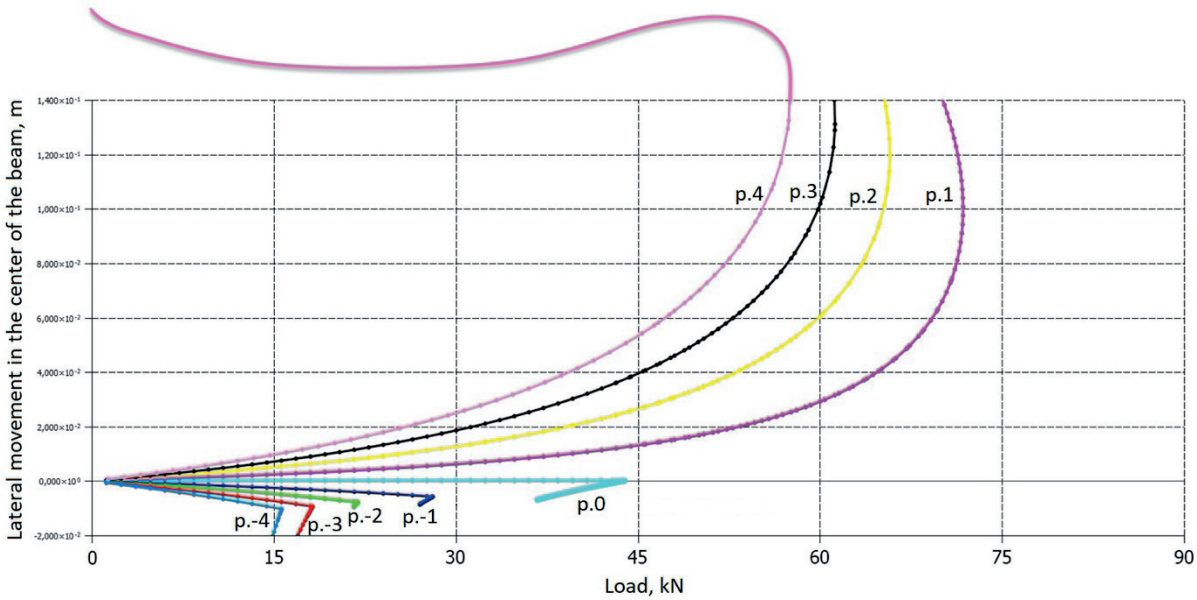

Figure 9. Deformation curves of symmetric angle bar (250 cm) under compression

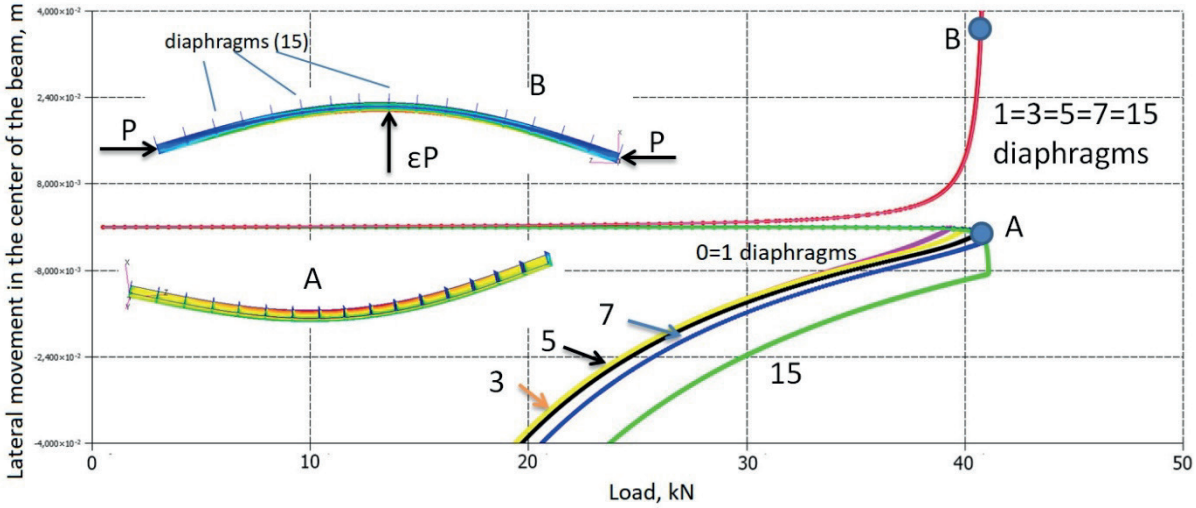

Figure 10. Deformation curves of symmetric angle bar (355 cm) with diaphragms under compression

However, with all the quantitative variants of the diaphragms (3, 5, 7, 15), the supercritical equilibrium was unstable and rather sharply decreasing in terms of the load. A small torque at the end of the beam was used as a disturbance. Under flexural disturbance by a small transverse force εP_1 (Fig. 10, edge in the compressed bending zone), the deflections developed up to the limiting point along the same curve, regardless of the diaphragms number. In general, the examined angle bar with diaphragms has an asymmetric bifurcation diagram.

In contrast, cantilever angle bars have a symmetrical stable post-bifurcation pattern up to the secondary bifurcation load (wave formation) in the flanges.

The Vlasov model of a thin-walled bar does not allow taking into account the actually observed contour deformation and secondary local wave formation in the profile flanges bifurcation effects.

We begin to study the features of equilibrium curves for cantilever beams by considering the stability problem for a steel cantilever beam 200 cm long with a cross-section in the form of a non-equilateral corner 3×2×0.3 cm (Fig. 11).

This rod has the first 5 bending eigenforms.

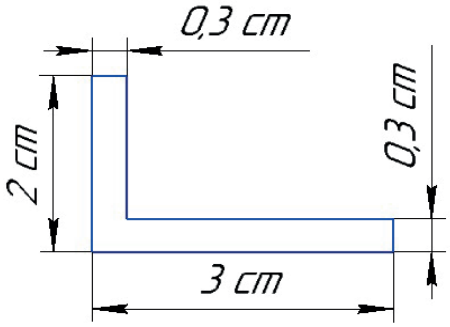

Figure 11. Cross-section of the cantilever beam

The compression load on the beam was applied as uniformly distributed over the end section of the free end. Solutions using the FEM (NASTRAN) showed that the bifurcation diagram of this cantilever rod is symmetric (the red and blue curves are the same and growing up to the moment of wave formation). Consequently, the post-critical equilibrium of such a beam is stable (Fig. 12) up to the moment of local wave formation near the bottom edge from the side of compressed fibers (Fig. 13). This wave formation is provoked by the interaction of two loss of stability forms: general and local. As soon as local wave formation occurs, the load reaches its maximum at the limiting point and then drops sharply (Fig. 12). It is clear that within the Vlasov model framework, the described forms interaction effect cannot be captured.

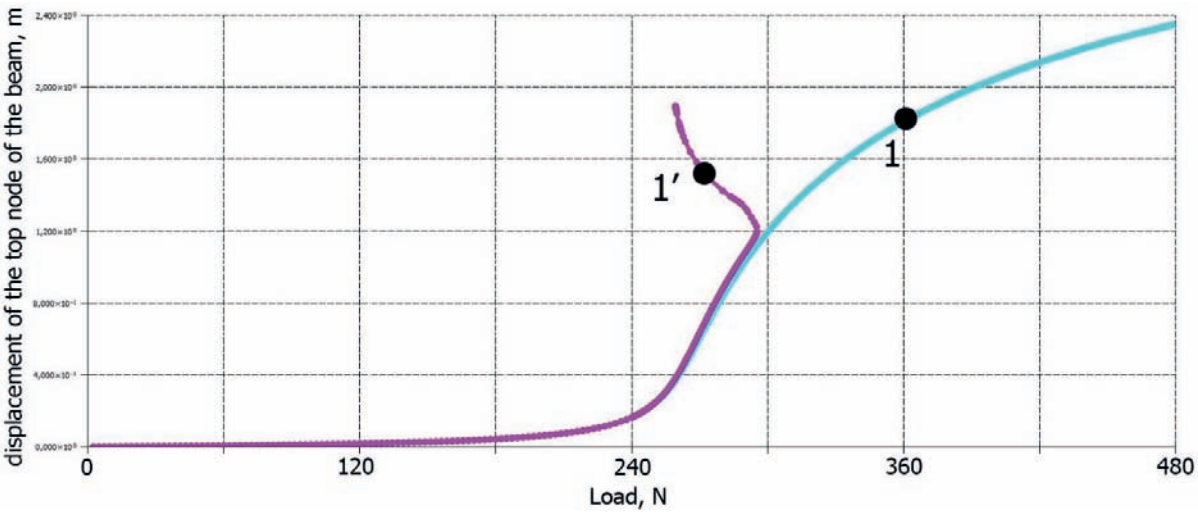

Figure 12. Deformation curves of fixed asymmetric angle bar (200 cm) under compression

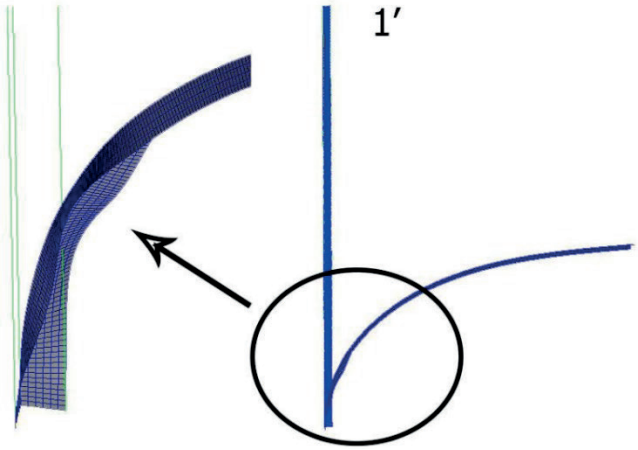

Figure 13. Local wave formation

Interesting results were obtained by the authors when calculating a compressed cantilever angle bar with a symmetric section of 10 ×10 ×0.3 cm and a length of 450 cm. The initial post-bifurcation equilibrium was stable up to the moment of wave formation in compressed flanges (point 1 in Fig. 14). At this point, a wave-like stress distribution is observed. Further, the equilibrium of the corner becomes unstable and the load drops sharply. If the transverse perturbation acts in the opposite direction (the flanges are stretched), then the equilibrium curve reaches the limiting point (point 1') along the same curve as in the first case.

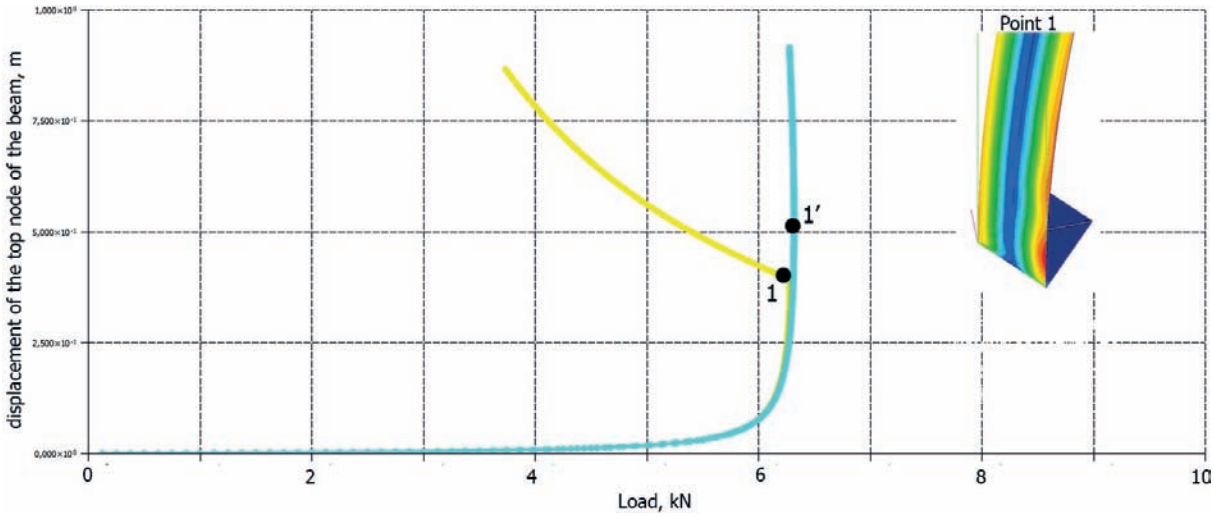

Figure 14. Deformation curves of fixed asymmetric angle bar (450 cm) under compression

Here, as in the previous example, before the waveform load, the bifurcation diagram of such a cantilever beam is symmetrical and stable (as opposed to hinged supported bars with an angle section).

Where does the limit point on the equilibrium curve come from? The authors believe that this is due to the deformation of the contour by the type of "flattening" of the angle bar near the bottom edge, where the greatest supercritical bending moment develops. Flattening reduces the bending stiffness of the corner section.

CONCLUSION

1. Compressed elastic thin-walled angle bars hinged at the ends have an asymmetric bifurcation diagram. Therefore they are extremely sensitive to bending imperfections, which cause additional compression of the zones located near the free edges of the flanges.
2. Compressed elastic cantilever beams of the angle bar have an initial post-bifurcation equilibria diagram that is symmetric and stable up to the load of wave formation in the flanges (secondary bifurcation, which is the result of the interaction of natural forms).
3. The energy theory of post-bifurcation behavior of the Vlasov thin-walled beam, constructed by M. Penyatoro and his collaborators, unfortunately, cannot capture all the important features (local wave formation, “flattening” of sections, etc.) of the development of supercritical stress-strain state of a real thin-walled beam.

REFERENCES

1. **Ilina A.A.** Prochnost i ustoychivost stal'nykh izgibayemykh elementov s regulyarnoy i neregulyarnoy shakhmatnoy perforatsiyey stenki: dissertatsiya na soiskaniye stepeni kand.tekhn. nauk: 05.23.01 / Ilina Anna Aleksandrovna. — Nizhniy Novgorod. – 2004.
2. **Mitchin R.B.** Mestnaya ustoychivost stenki i optimizatsiya stalnoy perforirovannoy balki: dissertatsiya na soiskaniye stepeni kand. tekhn. nauk: 05.23.01 / Mitchin Roman Borisovich. — Lipetsk. – 2003.
3. **Sinelnikov A.S.** Prochnost prosechno-rastyazhnogo profilya pri szhatii: dissertatsiya na soiskaniye stepeni kand. tekhn. nauk: 05.23.01 / Vatin N. I.. — Sankt-Peterburg. – 2015.
4. **Belyy G.I., Astakhov I.B.** Prostranstvennaya ustoychivost elementov konstruktsiy iz stal'nykh kholodnognutykh profiley // Montazhnyye i spetsialnyye raboty v stroitel'stve. — 2006. — Vol. 9.
5. **Tusnin A.R.** Chislennyy raschet konstruktsiy iz tonkostennykh sterzhney otkrytogo profilya.— Moskva: ASV. – 2009. — 143 p
6. **Crisan A., Ungureanu V., Dubina D.** Behaviour of cold-formed steel perforated sections in compression. Part 1— Experimental investigations. ThinWalled Structures. – 2012. – p. 86-96.
7. **Panovko Y.G., Gubanova I.I.** Ustoychivost i kolebaniya uprugikh sistem: Sovremennyye kontseptsii, paradoksy i oshibki. Stability and oscillations of elastic systems: Paradoxes, fallacies, and new concepts (in Russian). 6 ed. Moscow: KomKniga. – 2007.
8. **Vlasov V.Z.** Tonkostennyye uprugiye sterzhni. Moscow: Fizmatgiz. – 1959. – 574 p.
9. **Manuylov G.A., Begichev M.M.** On the reinforcement of thin-walled cold-drawn C-channel beams. IOP Conf. Series: Journal of Physics: Conf. Series. – 1425 (2020) . – 012031
10. **Pignataro M., Rizzi N., Luongo A.** Stability, Bifurcation and Postcritical Behaviour of Elastic Structures (Developments in Civil Engineering 39) Amsterdam: Elsevier Science. – 1991. – 355 p.
11. **Pignataro M., Gioncu V.** Phenomenological And Mathematical

Modelling Of Structural Instabilities. Wien; New York : Springer. – 2005. – 336 p.

СПИСОК ЛИТЕРАТУРЫ

1. **Ильина А.А.** Прочность и устойчивость стальных изгибаемых элементов с регулярной и нерегулярной шахматной перфорацией стенки: диссертация на соискание степени канд.техн. наук: 05.23.01 / Ильина Анна Александровна. — Нижний Новгород. – 2004.
2. **Митчин Р.Б.** Местная устойчивость стенки и оптимизация стальной перфорированной балки: диссертация на соискание степени канд. техн. наук: 05.23.01 / Митчин Роман Борисович. — Липецк. – 2003.
3. **Синельников А.С.** Прочность просечно-растяжного профиля при сжатии: диссертация на соискание степени канд. техн. наук: 05.23.01 / Ватин Н. И.. — Санкт-Петербург. – 2015.
4. **Белый Г.И., Астахов И.Б.** Пространственная устойчивость элементов конструкций из стальных холодногнутых профилей. Монтажные и специальные работы в строительстве. — 2006. — Т. 9.
5. **Туснин А.Р.** Численный расчет конструкций из тонкостенных стержней открытого профиля.— Москва: АСВ. – 2009. — 143 с
6. **Crisan A., Ungureanu V., Dubina D.** Behaviour of cold-formed steel perforated sections in compression. Part 1— Experimental investigations. ThinWalled Structures. – 2012. – p. 86-96.
7. **Пановко Я.Г., Губанова И.И.** Устойчивость и колебания упругих систем. Современные концепции, парадоксы и ошибки. 6-е издание. М.: КомКнига. – 2007.
8. **Власов В.З.** Тонкостенные упругие стержни. М.: Физматгиз. – 1959. – 574 с.
9. **Manuylov G.A., Begichev M.M.** On the reinforcement of thin-walled cold-drawn C-channel beams. IOP Conf. Series: Journal of Physics: Conf. Series. – 1425 (2020) . – 012031
10. **Pignataro M., Rizzi N., Luongo A.** Stability, Bifurcation and Postcritical Behaviour of Elastic Structures (Developments in Civil Engineering 39) Amsterdam: Elsevier Science. – 1991. – 355 p.
11. **Pignataro M., Gioncu V.** Phenomenological And Mathematical Modelling Of Structural Instabilities. Wien; New York : Springer. – 2005. – 336 p.

Gaik A. Manuylov, Ph.D., Associate Professor, Department of Structural Mechanics, Russian University of Transport; 127994, Russia, Moscow, 9b9 Obrazcova Street; phone/fax +7(499)972-49-81.

Sergey B. Kosytsyn, Dr.Sc., Professor, Head of Department of Theoretical Mechanics, Russian University of Transport; 127994, Russia, Moscow, 9b9 Obrazcova Street; phone/fax: +7(499) 978-16- 73; E-mail: kositsyn-s@yandex.ru, kositsyn-s@mail.ru

Maxim M. Begichev, Ph.D., Associate Professor, Department of Theoretical Mechanics, Russian University of Transport; 127994, Russia, Moscow, 9b9 Obrazcova Street; phone/fax: +7(499) 978-16-73; E-mail: noxonius@mail.ru

Мануйлов Гайк Александрович, кандидат технических наук, доцент, доцент кафедры «Строительная механика» Российского университета транспорта; 127994, г. Москва, ул. Образцова, 9, стр. 9; тел./факс +7(499) 972-49-81

Косицын Сергей Борисович, доктор технических наук, профессор, заведующий кафедрой «Теоретическая механика» Российского университета транспорта; 127994, г. Москва, ул. Образцова, 9, стр. 9; тел./факс +7(499) 978-16-73; E-mail: kositsyn-s@yandex.ru, kositsyn-s@mail.ru

Бегичев Максим Михайлович, кандидат технических наук, доцент кафедры «Теоретическая механика» Российского университета транспорта; 127994, г. Москва, ул. Образцова, 9, стр. 9; тел./факс +7(499) 978-16-73; E-mail: noxonius@mail.ru